



Earth reflectance and polarization intercomparison between SCIAMACHY onboard Envisat and POLDER onboard ADEOS-2

L. G. Tilstra¹ and P. Stammes¹

Received 29 June 2006; revised 4 December 2006; accepted 13 January 2007; published 8 June 2007.

[1] In this paper, we compare reflectance and polarization measurements from two different satellite instruments, namely, the imager Polarization and Directionality of the Earth's Reflectances (POLDER) and the spectrometer Scanning Imaging Absorption Spectrometer for Atmospheric Chartography (SCIAMACHY). Both instruments are able to measure not only the Earth reflectance but also the state of linear polarization of the detected light. The aim of this paper is to validate the SCIAMACHY reflectance and polarization data using the fact that POLDER is well calibrated. This validation requires a careful search for suitable, collocated data having identical solar and viewing angles. For the reflectance, there is a disagreement between POLDER and SCIAMACHY of up to 20% in the wavelength interval 400–1000 nm, which we attribute to SCIAMACHY. As for the linear polarization, we present for the first time clear evidence for the existence of discrepancies in the SCIAMACHY polarization retrieval for polarization measurement devices 2, 3, and 4.

Citation: Tilstra, L. G., and P. Stammes (2007), Earth reflectance and polarization intercomparison between SCIAMACHY onboard Envisat and POLDER onboard ADEOS-2, *J. Geophys. Res.*, *112*, D11304, doi:10.1029/2006JD007713.

1. Introduction

[2] Spectrometry of the Earth's atmosphere in the short-wave spectral range (from the ultraviolet to the near-infrared) has received much attention with the availability of data from Global Ozone Monitoring Experiment (GOME), launched in April 1995 onboard the ERS-2 satellite, and Scanning Imaging Absorption Spectrometer for Atmospheric Chartography (SCIAMACHY), launched in March 2002 onboard the Envisat satellite. These instruments, which have a spectral resolution of about 0.2–1.5 nm, have enabled chemical composition measurements of the atmosphere down to the surface. Important trace gases like O₃, NO₂, BrO, H₂CO, SO₂, and H₂O, and, with SCIAMACHY, also CO and CH₄, as well as clouds and aerosols, have been detected globally with these instruments [Burrows *et al.*, 1999; Bovensmann *et al.*, 1999; Gottwald *et al.*, 2006].

[3] The Earth reflectance at top-of-atmosphere (TOA) is a basic quantity for all geophysical products derived from GOME and SCIAMACHY. Both instruments measure the Earth radiance as well as the solar irradiance at TOA, so the reflectance can be determined from their ratio. The advantage of working with the reflectance is that several uncertainties in the radiance and irradiance cancel out. The instrument's radiometric calibration of radiance and irradiance is the most important factor determining the quality of the reflectance, and of the derived geophysical products. Some products, like the column densities of most trace gases, which are usually retrieved by the differential optical

absorption spectroscopy (DOAS) method [Platt, 1994], are insensitive to errors in the absolute calibration of the reflectance. Other products, however, like the vertical distribution of ozone [Munro *et al.*, 1998; Hoogen *et al.*, 1999; Spurr, 2001; van der A *et al.*, 2002; Hasekamp *et al.*, 2002; Meijer *et al.*, 2003], cloud properties [Koelemeijer *et al.*, 2001; Acarreta *et al.*, 2004], and aerosol properties [de Graaf and Stammes, 2005], rely strongly on a correct absolute calibration of the reflectance.

[4] In the first year after the launch of SCIAMACHY [Bovensmann *et al.*, 1999], a number of studies showed indications of severe shortcomings in its radiometric calibration [see, e.g., Skupin *et al.*, 2003; Acarreta and Stammes, 2003]. The shortcomings in the reflectance calibration were confirmed later on for the UV by comparison with radiative transfer models [van Soest *et al.*, 2005; Tilstra *et al.*, 2005] and for visible and near-infrared wavelength ranges by comparison with the satellite instruments Medium-Resolution Imaging Spectrometer (MERIS) and GOME [Acarreta and Stammes, 2005; von Hoyningen-Huene *et al.*, 2006; Tilstra and Stammes, 2006]. Most notable was the 15–25% underestimation of the reflectance by SCIAMACHY. Although this problem was partly removed with the calculation of alternative instrument response data, some negative side effects were introduced in the process, such as the occurrence of spectral features in the reflectance, which could potentially harm DOAS retrievals. Additionally, the reflectance spectra are still troubled by the existence of polarization features caused by errors in the retrieved linear polarization [Tilstra and Stammes, 2005]. In summary, the quality of the SCIAMACHY reflectance is still far from the level that had been anticipated before launch (reflectance accurate within 1%).

¹Royal Netherlands Meteorological Institute, De Bilt, The Netherlands.

Table 1. Specifications of SCIAMACHY's Eight Spectral Channels and Seven Broadband Polarization Measurement Devices (PMDs)^a

Channel	Spectral Range (nm)	Resolution (nm)
1	240–314	0.24
2	309–405	0.26
3	394–620	0.44
4	604–805	0.48
5	785–1050	0.54
6	1000–1750	1.48
7	1940–2040	0.22
8	2265–2380	0.26

PMD	Spectral Range (nm)	Sensitive to
1	310–377	Q
2 ^a	450–525	Q
3 ^a	617–705	Q
4 ^a	805–900	Q
5	1508–1645	Q
6	2265–2380	Q
7	802–905	U

^aThe PMDs that are relevant to this paper.

[5] The first aim of this paper is to validate the SCIAMACHY reflectance by making use of the imager Polarization and Directionality of the Earth's Reflectances (POLDER) [Deschamps *et al.*, 1994] as a reliable reference. POLDER has a calibration accuracy better than 2% for the reflectance [Hagolle *et al.*, 1999] and has a unique multi-directional measurement approach which allows it to mimic the SCIAMACHY observational geometry. By this comparison with POLDER, we can also extend the wavelength range of the SCIAMACHY reflectance validation further into the near-infrared.

[6] The second aim is to validate the polarization retrieval algorithm (PRA) of SCIAMACHY by comparison with POLDER polarization measurements of the Earth as a reference. POLDER measures the state of polarization with an accuracy of 0.01 or better [Toubbé *et al.*, 1999]. The main task of the SCIAMACHY PRA is to calculate, from the signals of the polarization measurement devices (PMDs) and the spectral channels, the Stokes parameters Q and U [van de Hulst, 1981] that describe the (linear) polarization of the incident radiation [Slijkhuis, 2001]. The performance of the PRA is very relevant to the quality of the Earth reflectance because, as most spectrometers, SCIAMACHY is sensitive to the state of polarization of the detected radiation. The polarization correction algorithm needs reliable polarization values from the PRA to correct for this dependence on polarization.

[7] Validation of atmospheric polarization measurements is a complicated task, and there are only a small number of techniques available. The first validation method that deserves attention is a method that focuses on special situations where the viewing and solar geometry of the problem is such that the detected light is unpolarized, regardless of the actual atmospheric situation [Aben *et al.*, 2003]. The disadvantage of this method is that these special cases occur only twice per viewing angle per orbit, and that the method is by definition restricted to unpolarized cases. A second method, baptized as the method of limiting atmospheres [Krijger *et al.*, 2005], makes use of a limit of maximum polarization that is reached by a large collection of cloud-free situations. The disadvantage of this method is

that it requires a long record of data, and, more importantly, the polarization limit found in this way is instrument-dependent. For an absolute validation, the method cannot be used. Nevertheless, both methods have already proved to be very useful for precise monitoring of degradational effects in GOME, where the restrictions of the methods are of minor importance. In the present study, we will be comparing polarization data of SCIAMACHY and POLDER directly, in such a way that we can validate in an absolute sense the SCIAMACHY polarization observations.

[8] Earlier validation studies of SCIAMACHY polarization have been limited to verification, by considering if the values are physically possible [Krijger and Tilstra, 2003], and to validation in the UV by an alternative polarization retrieval algorithm [Tilstra and Stammes, 2005], which showed that the operational polarization retrieval algorithm worked quite well for PMD 1 (~344 nm). However, an accurate validation of the polarization values of the other PMDs (at larger wavelengths) was still lacking. In this paper, we will be presenting the first validation results for PMDs 2, 3, and 4.

[9] The outline of this paper is as follows. In section 2, we briefly introduce the satellite instruments POLDER and SCIAMACHY. Section 3 explains the approach that was followed to perform an accurate intercomparison between the level-1 data of these two satellite instruments. Section 4 presents the results of this intercomparison, for the Earth reflectance and for the Earth polarization. The results are discussed and linked to results of other recent studies. The paper ends with a summary and conclusion.

2. Satellite Instruments Description

2.1. Description of SCIAMACHY

[10] SCIAMACHY [Bovensmann *et al.*, 1999] is a spectrometer designed to measure sunlight reflected by the Earth's atmosphere over the wavelength range 240–2380 nm, with a spectral resolution of 0.22–1.48 nm (cf. Table 1). The instrument was launched on 1 March 2002 onboard the European Envisat satellite, which is in a near-polar, Sun-synchronous orbit. The local time of the equator crossing is 10:00 a.m. for the descending node and the orbital period is about 100 min. An overview of all available scientific products from SCIAMACHY is given at <http://www.sciamachy.org/validation/>.

[11] SCIAMACHY has the ability to perform measurements in either nadir or limb mode. This is a new aspect as compared to its predecessor GOME [Bovensmann *et al.*, 1999], which only has a nadir mode. The two measurement modes are normally being alternated along the orbit, and the collected data are stored in blocks called "states." Since our aim is to intercompare SCIAMACHY level-1 data with POLDER level-1 data, we will only make use of the nadir mode of the instrument. The size of a typical nadir state is approximately 960×490 km (across track \times along track). This area is scanned in the along-track direction by virtue of the forward movement of the satellite and in the across-track direction as a result of an internal mirror scanning back (eastward in 1 s) and forth (westward in 4 s) every 5 s. In this way, global coverage of the planet in nadir mode is achieved in roughly 6 days.

Table 2. Overview of the POLDER Spectral Bands^a

POLDER Band	443	443P	490	565	670P	763	765	865P	910
Central Wavelength, nm	444.9	444.5	492.2	564.5	670.2	763.3	763.1	860.8	907.7
Bandwidth, nm	20	20	20	20	20	10	40	40	20
Saturation Level (norm. reflectance)	0.97	1.1	0.75	0.48	1.1	1.1	1.1	1.1	1.1
Polarization (Q , U)	–	Yes	–	–	Yes	–	–	Yes	–
SCIAMACHY PMD Band		2			3			4	
Central Wavelength, nm		487			661			853	
Bandwidth, nm		75			88			95	

^aAll POLDER bands are well within the SCIAMACHY spectral range. Also given are specifications for the SCIAMACHY PMDs that are comparable to the POLDER polarization bands. A graphical representation of the spectral response functions of the POLDER bands is given in Figure 2.

[12] To have as small as possible ground pixels within a limited data rate, SCIAMACHY employs a variable integration time (IT) within the recorded spectra. The spectrum, for this purpose, has been divided into specific wavelength regions, called “clusters,” which can be read out with different ITs. This allows a higher spatial resolution for clusters that contribute much to the retrieval of the trace gases at the expense of clusters that in their current use offer little or no atmospheric information. Next to that, the ITs of the clusters can be changed along the orbit (per state) to prevent saturation or too low signals. In the nadir mode of the instrument, 56 of such clusters exist, usually with integration times of 0.25 or 1.0 s, although other ITs are also possible. The two mentioned ITs correspond to nadir pixel sizes of 60×30 km and 240×30 km, respectively.

[13] The spectral detectors of SCIAMACHY are sensitive to the state of polarization of the incident light. To be able to correct for this sensitivity, which has been characterized preflight for Stokes parameters Q and U , polarization is measured at six different wavelengths using seven broadband PMDs. The Q and U sensitivities of the PMDs have also been characterized preflight. The specifications of the PMDs are listed in Table 1. PMDs 1–6 are mostly sensitive to the Stokes parameter Q , and all measure the radiance component I_{\perp} perpendicular to the entrance slit, and not so much the component I_{\parallel} parallel to the entrance slit. This alone is not enough to calculate $Q = I_{\parallel} - I_{\perp}$, but the radiance signals of the main channels can be used to provide additional information through $I = I_{\parallel} + I_{\perp}$. This method has worked well in the past for the spectrometer GOME [Aben *et al.*, 2003]. For PMD 7, which is sensitive to the Stokes parameter U , a similar approach is followed [Slijkhuis, 2001].

2.2. Description of POLDER

[14] The first POLDER instrument [Deschamps *et al.*, 1994] was launched in August 1996 onboard the Japanese Advanced Earth Observing Satellite (ADEOS) and operated until 30 June 1997. The scientific goal of POLDER was to contribute to climate-related research by determining the influence of aerosols and clouds on the Earth radiation budget and by studying the ocean and land surface properties, particularly vegetation. The second, identical version of the instrument was launched into orbit on the ADEOS-2 satellite in December 2002 and operated until 25 October 2003. The ADEOS-2 satellite was in a near-polar, Sun-synchronous orbit with an orbital period of approximately 100 min. The local time of the equator crossing was 10:30 a.m. for the descending node.

[15] The POLDER instrument was designed to measure the first three parameters of the Stokes vector [van de Hulst, 1981], so that the instrument did not only record the Earth radiance I but also the state of linear polarization of the backscattered sunlight described by the Stokes parameters Q and U . The POLDER measurement principle is based on a bidimensional charge-coupled device (CCD) detector, a rotating wheel carrying 15 optical filters and polarizers, and a wide field-of-view telecentric optics which projects the light onto the CCD detector array. Thanks to the available spectral filters and polarizers, measurements of I can be performed within nine spectral bands (see Table 2). For three of these spectral bands, Stokes parameters Q and U are measured as well.

[16] An important and unique feature of the POLDER design is the fact that the measurements are repeated (every 19.6 s) in such a way that an image of an Earth scene overlaps largely with the previous image (see Figure 1a). As a result, a given point inside the POLDER swath may be observed by as much as 14 independent measurements, each having a different viewing geometry and thus a different scattering angle. This capability allows studying scattering-angle-dependent phenomena, like rainbows and glories, which are important to determine size and shape of aerosol and cloud properties. The pixel size of a POLDER image is about 6×7 km at exact nadir. The instrument’s swath is 2400 km, and viewing angles up to 70° are reached (cf. Figure 1b). As a result, global coverage of the Earth’s surface is achieved virtually on a daily basis.

3. Intercomparison Approach

[17] The reflectance in this paper is defined as

$$R = \frac{\pi I}{\mu_0 E}, \quad (1)$$

where I is the radiance reflected by the Earth atmosphere (in $\text{W m}^{-2} \text{nm}^{-1} \text{sr}^{-1}$), E is the incident solar irradiance at the top of the atmosphere perpendicular to the solar beam (in $\text{W m}^{-2} \text{nm}^{-1}$), and μ_0 is the cosine of the solar zenith angle θ_0 . To intercompare the reflectance and polarization data of both instruments, collocations should be found, and scattering geometries of collocated measurement data should be identical.

3.1. Spatial and Temporal Collocation

[18] Collocation in this case means that both satellites follow the same orbit track, i.e., reach each other’s subsat-

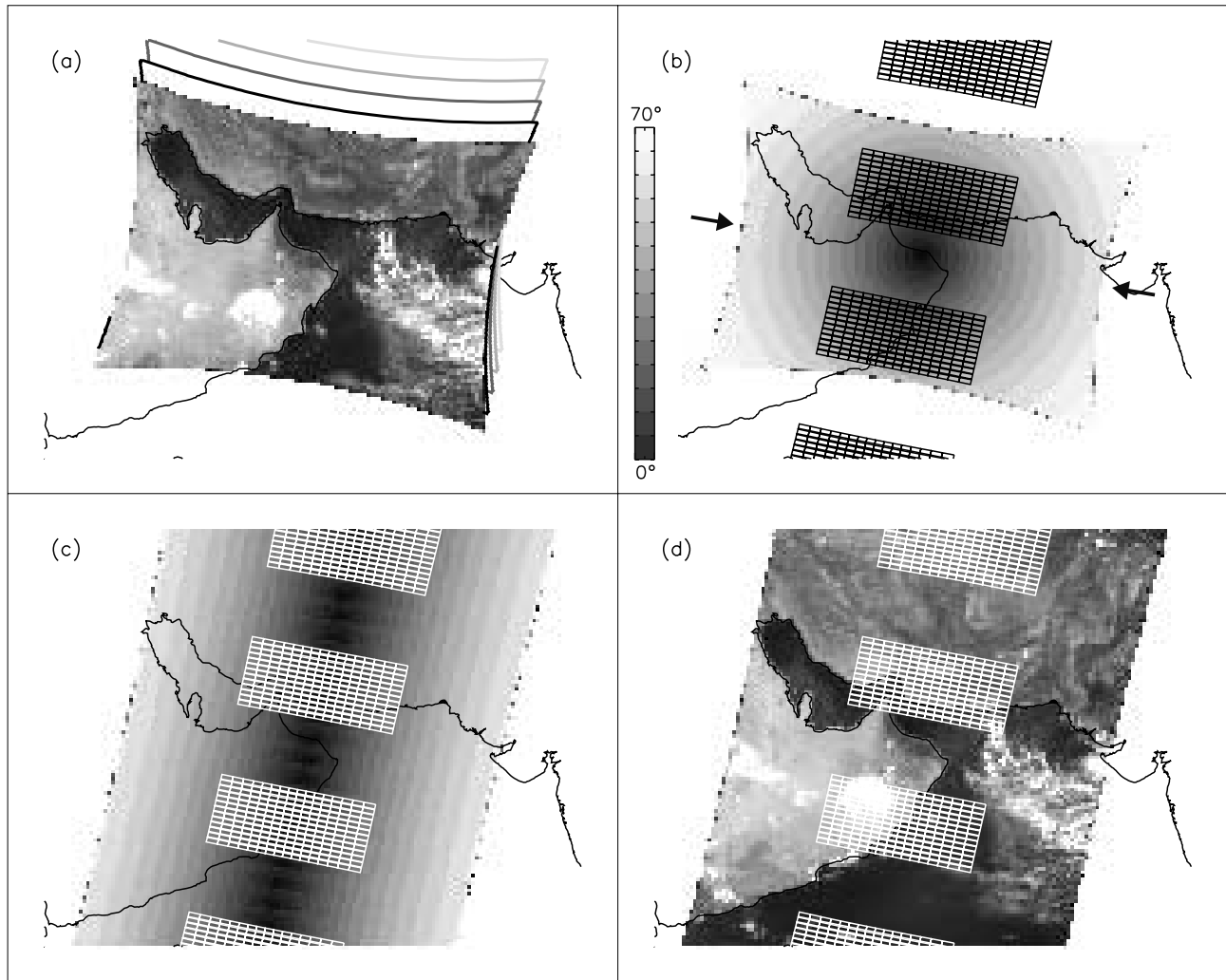


Figure 1. (a) Single reflectance image of the area containing the Arabian peninsula and surrounding seas (58°N , 23°E) measured by the POLDER 670-nm spectral channel, and contours of previous images. (b) Viewing angles of the POLDER data and contours of SCIAMACHY (forward scan) pixels of 0.25-s IT. (c) We select from each POLDER image a subset of data with viewing directions that best approach SCIAMACHY's scanning directions from east to west. Here, the viewing angles of all these subsets are plotted. (d) For the same collection of subsets, we plot the 670-nm reflectance measured by POLDER.

ellite point with a time difference of only about 30 min. For the moment we assume that changes in the observed scene during this small time difference, for example, because of movement of clouds, are small. Because of differences in the orbital periods of the ADEOS-2 and Envisat satellites, collocation in the strict way we defined it only takes place once in about 15 days. For this paper, we selected a scene covered by SCIAMACHY orbit 7503 (software version 5.01) and POLDER-2 orbit 060/048 (software version 14.01) of 7 August 2003. Part of this scene is illustrated in Figure 1d.

3.2. Scattering Geometry

[19] The scattering geometry is determined by the viewing geometry of the satellite instrument, represented by the angles θ and ϕ , and the position of the Sun, represented by the angles θ_0 and ϕ_0 . As for the viewing geometry, Figure 1b illustrates the fundamental difference between the viewing geometry of both instruments. POLDER, by virtue of its wide

field-of-view telecentric optics, observes the Earth in all azimuth directions, while SCIAMACHY scans the Earth's surface perpendicular to the flight direction, from east to west, and back along the same azimuthal direction ϕ .

[20] To ensure comparable viewing geometries, we have to filter out those POLDER data that have different azimuth directions than the SCIAMACHY data. This leaves us with only a small strip of POLDER data with suitable azimuth angles, indicated by the arrows in Figure 1b. All individual POLDER measurement events (images) contribute such a strip of data; the resulting collection of viewing angles is illustrated in Figure 1c. The viewing angles of this selection of POLDER data closely resemble those of the SCIAMACHY instrument because both satellites are in a similar orbit.

[21] At this point we should mention that, because of the difference in overpass time of the ADEOS-2 and Envisat satellites, the solar angles of POLDER and SCIAMACHY are slightly different. The difference is depending on orbit

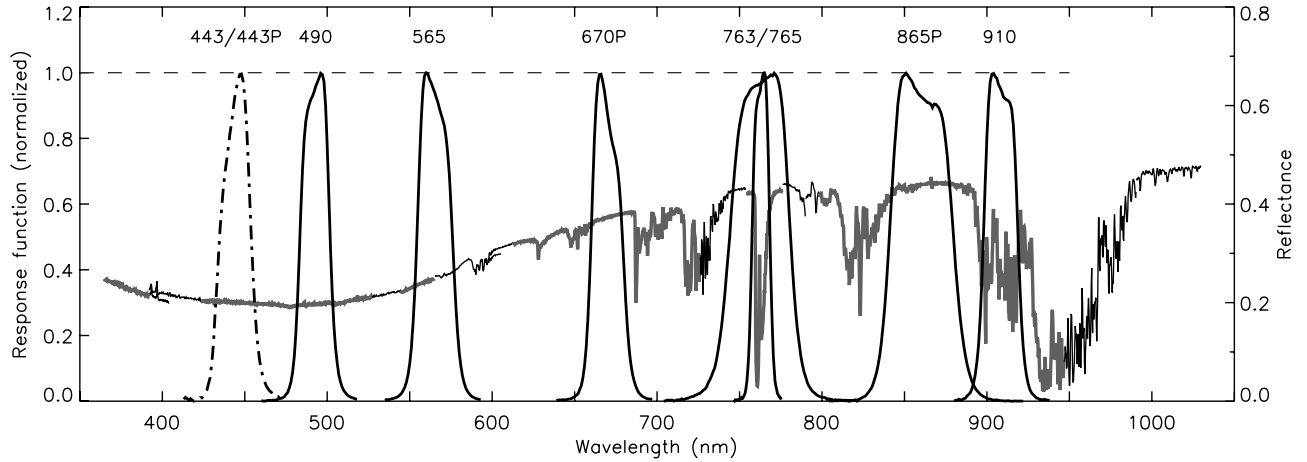


Figure 2. Spectral response functions of the POLDER spectral bands (left axis) and a SCIAMACHY reflectance spectrum of a desert scene (right axis). Where the reflectance curve is thick, the integration time (IT) of the SCIAMACHY wavelength clusters is 0.25 s, and the reflectance is the average of four subsequent measurements. Elsewhere, the IT is 1.0 s.

phase and can reach up to 7° for the solar zenith angle θ_0 . The effect of this on the reflectance is small, namely, less than 1% in the reflectance [cf. *Tilstra and Stammes, 2006*]. For the quantities Q/I and U/I describing the linear polarization, we found from radiative transfer simulations a somewhat higher estimated effect. The maximum deviation, found for the highest difference in θ_0 , and over ocean surface, was ~ 0.02 at 450 nm to ~ 0.01 at 900 nm. Note that in most other cases, the errors are much smaller.

3.3. Spatial Averaging

[22] Dealing with the different pixel sizes of POLDER and SCIAMACHY is relatively easy because the pixel sizes of the two instruments are so different (6×7 km for POLDER versus 60×30 km or 240×30 km for SCIAMACHY). Starting out with a SCIAMACHY pixel, we collect all suitable POLDER pixels of which the centers lie within the SCIAMACHY pixel. We then average the collected POLDER reflectances, which are denoted as R_i^p , to obtain \bar{R}_i^p . Here the superscript p refers to the POLDER instrument, while i refers to the spectral band in question. We do the same for the collected Stokes parameters, which are denoted as Q_i^p and U_i^p . Doing so, we arrive at the spatially averaged quantities \bar{R}_i^p , \bar{Q}_i^p , and \bar{U}_i^p . This procedure is repeated for all spectral bands i . Depending on the IT and pixel size of the SCIAMACHY pixels, there are ~ 50 (IT = 0.25 s) or ~ 200 (IT = 1.0 s) POLDER pixels inside every single SCIAMACHY pixel.

3.4. Reflectance: Spectral Equivalents

[23] POLDER and SCIAMACHY are spectrally fundamentally different. POLDER is an imager, in which the radiance signals are determined by nine broadband detectors. This results in nine broadband reflectances R_i^p , where i refers to the spectral band in question. SCIAMACHY, on the other hand, retrieves a full, continuous reflectance spectrum $R^s(\lambda)$. This is illustrated graphically in Figure 2, which shows the response functions of the POLDER broadband detectors and part of a reflectance spectrum measured by SCIAMACHY over a desert scene. Note the jumps in the reflectance around 400, 600, and 800 nm. They

are related to calibration problems in the channel overlap regions. These jumps are fortunately located outside the range of the POLDER broadband detectors and therefore pose no threat to the reflectance intercomparison.

[24] Along with knowledge of the response functions of the POLDER spectral bands, it is possible to integrate the SCIAMACHY spectral reflectance to a POLDER-equivalent reflectance R_i^s :

$$R_i^s = \int_0^\infty s_i(\lambda) R^s(\lambda) d\lambda, \quad (2)$$

where s_i is the response function of the i th POLDER band and λ stands for the wavelength. Strictly speaking, we have made an error in equation (2) because we should not integrate the reflectance, but instead integrate the radiance and irradiance separately, and then use equation (1) to calculate R_i^s . The error that is introduced in this way is, however, very small as the irradiance is relatively constant over the narrow POLDER bandwidths over which is being integrated.

[25] Inspecting Figure 2 reveals that there are complications for POLDER reflectances R_{565}^p and R_{765}^p . For these two bands, not all the covered SCIAMACHY wavelength clusters are read out with the same IT of 0.25 s (and hence the pixel sizes are different). This problem can be solved by combining four subsequent SCIAMACHY measurements with an IT of 0.25 s to simulate one measurement of 1.0 s IT for those clusters that were read out with 0.25 s IT. In this way, one is able to construct a complete reflectance spectrum for an IT of 1.0 s, which can be integrated according to equation (2), albeit at a lower spatial and temporal resolution than for the other POLDER bands, which only cover SCIAMACHY clusters with an IT of 0.25 s. This approach was applied to obtain R_{565}^s and R_{765}^s . For the other spectral bands, an IT of 0.25 s was available.

3.5. Polarization: Comparable Bands

[26] For the intercomparison of the Earth polarization, we used the following strategy. From the POLDER polarization data product, the Stokes parameter ratios \bar{Q}_i^p/\bar{I}_i^p , and \bar{U}_i^p/\bar{I}_i^p

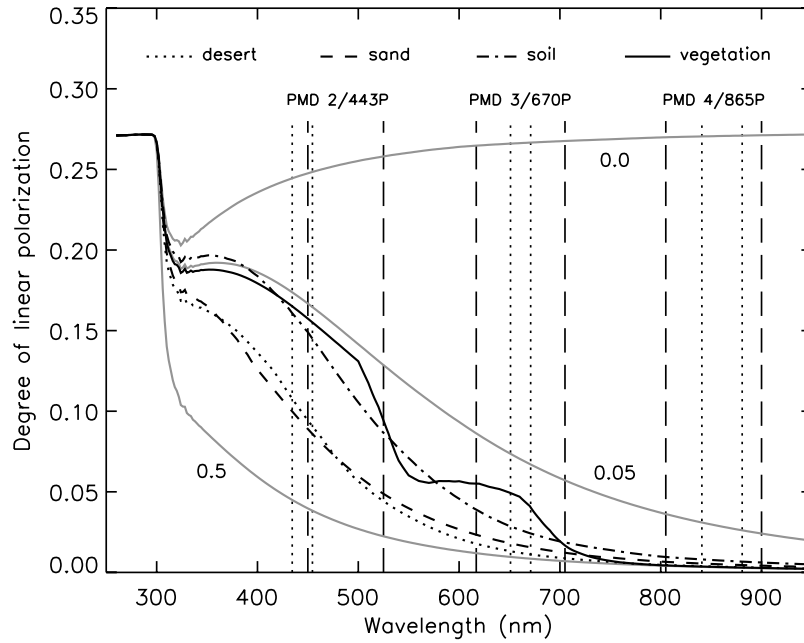


Figure 3. Spectral variation of the TOA degree of linear polarization for four different surface types, indicated by the legend, and for three wavelength independent surface albedos of 0, 0.05, and 0.5, indicated by the gray solid curves. The curves were calculated by the radiative transfer model DAK, for $\theta = 9^\circ$, $\theta_0 = 35^\circ$, $\phi - \phi_0 = -45^\circ$. The surfaces were assumed to be depolarizing. The vertical lines indicate the sensitivity ranges of SCIAMACHY PMDs 2–4 (dashed lines) and the three POLDER polarization bands (dotted lines).

were calculated for the three polarization spectral bands at 443, 670, and 865 nm (see Table 2). From these we calculated the POLDER degree of linear polarization:

$$\bar{P}_i^p = \sqrt{(\bar{Q}_i^p/\bar{I}_i^p)^2 + (\bar{U}_i^p/\bar{I}_i^p)^2}. \quad (3)$$

The reasons for also studying this parameter P are (1) it is a more intuitive parameter than Q and U , and (2) it is not depending on the reference plane like Q and U , and therefore less sensitive to remaining differences between the viewing and solar angles of both instruments. Note in this respect that polarization is more sensitive to scattering geometry than reflectance.

[27] The values of \bar{Q}_i^p/\bar{I}_i^p , \bar{U}_i^p/\bar{I}_i^p , and \bar{P}_i^p are considered to be equivalents of the Stokes parameter ratios and the degree of linear polarization calculated from the SCIAMACHY polarization measurements performed by PMDs 2, 3, and 4 (cf. Table 2). As can be concluded from Table 2, there are small differences in the central wavelength and bandwidth of the POLDER and SCIAMACHY polarization bands. The effects of these differences will be discussed in section 3.6.

3.6. Polarization: Spectral Mismatch

[28] The spectral response functions of the SCIAMACHY PMDs and the POLDER polarization bands are not the same. We will now try to provide a rough estimate of the consequences of this spectral mismatch for the polarization comparison presented in section 4.2.

[29] Figure 3 presents some calculations of the TOA degree of linear polarization, presented as a function of

wavelength, for a number of surface types. These surface types include “desert,” “sand,” “soil,” and “vegetation” (from *Bowker et al.* [1985]) and have a spectrally varying albedo, as well as three artificial surfaces with constant albedos of 0, 0.05, and 0.5. The calculations were performed by the radiative transfer model Doubling-Adding KNMI (DAK) [*de Haan et al.*, 1987; *Stammes*, 2001] for typical viewing and solar angles taken from the scene shown in Figure 1. The surface was assumed to be Lambertian, i.e., completely depolarizing. Aerosols and clouds were not included in the simulations.

[30] Clearly, the TOA degree of linear polarization is strongly influenced by the surface type in the model and shows a strong wavelength dependence. Also, given in Figure 3 are vertical lines that indicate the sensitivity ranges of the SCIAMACHY PMDs (dashed lines) and the POLDER polarization bands (dotted lines). The spectral mismatch is the largest for PMD 2/443P. Judging from Figure 3, POLDER band 443P would record a higher degree of linear polarization than SCIAMACHY PMD 2, by about 0.01–0.03, depending on the surface type.

4. Results of the Intercomparison

4.1. Reflectance

[31] The main result for the reflectance intercomparison between POLDER and SCIAMACHY is shown in Figure 4. On the vertical axis, we plot the POLDER reflectances \bar{R}_i^p , for all nine POLDER spectral bands i ; on the horizontal axis, we plot their SCIAMACHY equivalents \bar{R}_i^s , calculated using equation (2). The \bar{R}_i^p mentioned here are the spatially averaged values as described in section 3.3. The intercom-

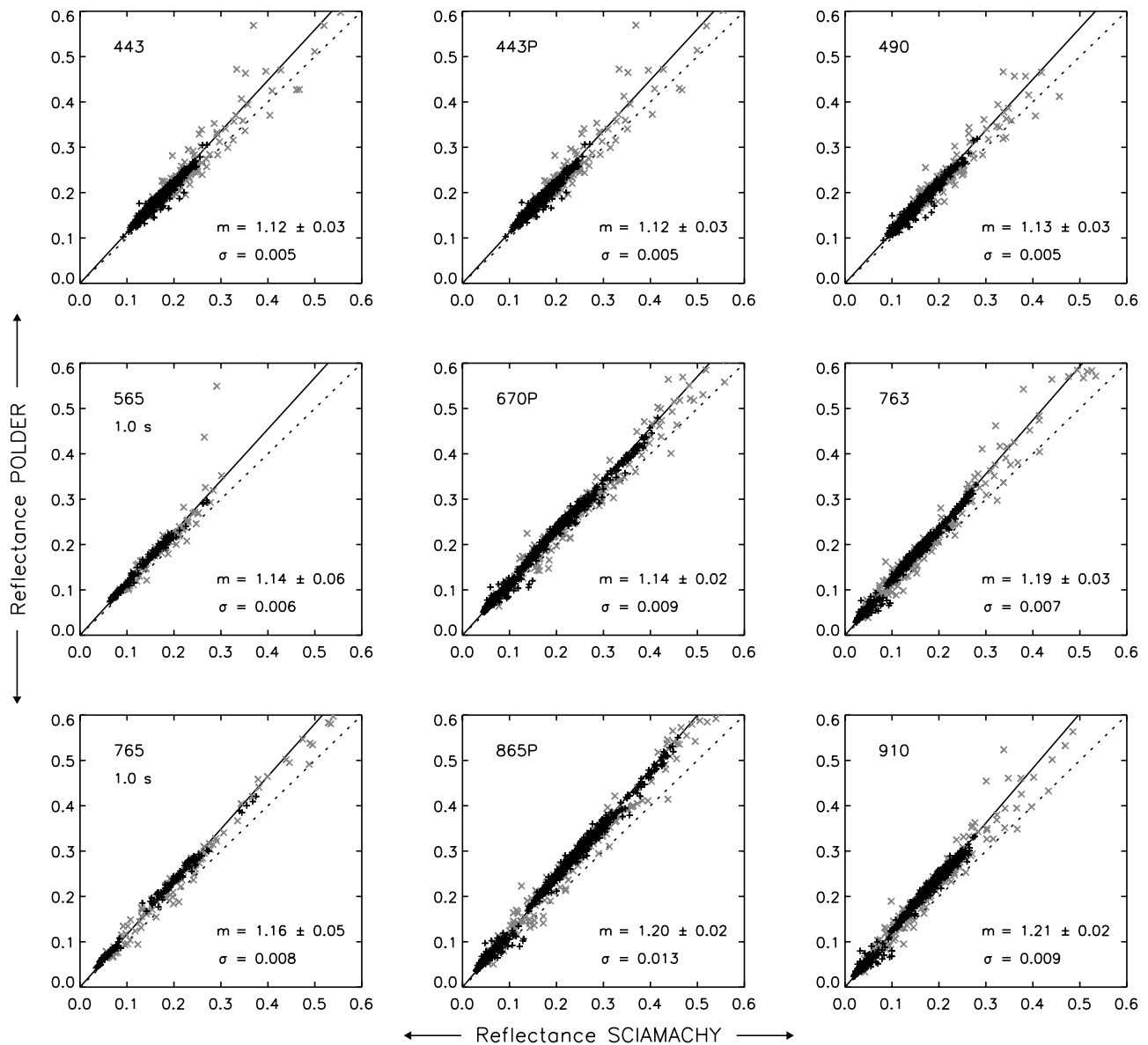


Figure 4. Result of the reflectance comparison: POLDER versus SCIAMACHY, for all nine POLDER bands. The gray crosses are flagged as cloudy pixels, and the black pluses as being cloud-free. The dotted line indicates the one-to-one relationship. The solid line represents the one-parameter linear fit to the cloud-free data. Its slope m is given, along with σ , the spread in the data. Note that the results for POLDER spectral bands 565 and 765 were determined for the SCIAMACHY integration time of 1.0 s (instead of 0.25 s).

parison was done for 1040 SCIAMACHY forward scan pixels (5 nadir states), of which 807 were labeled cloud-free. Backscan pixels were not included in the analysis. In Figure 4, the cloudy pixels are indicated with gray crosses, cloud-free pixels with black pluses. The specific differences between the two types of pixels will be discussed later on. A linear one-parameter fit to the cloud-free data is also shown. Its slope m is given along with the standard deviation σ representing the spread of the data.

[32] As can be seen, the correlation between the POLDER and SCIAMACHY reflectances is linear, but there appears to be a systematic deviation from the one-to-one line. A possible viewing-angle dependency, either for the POLDER

or SCIAMACHY data, was not found. Other dependencies, such as scene dependencies, or latitude/longitude dependencies, were not found either. In particular, the effect of scene inhomogeneity could be studied by discriminating between cloudy and cloud-free pixels. Cloudy pixels, in this case, are pixels that are reported cloudy by POLDER and/or SCIAMACHY. These pixels may be inhomogeneous, and their reflectances are likely to vary during the time interval between POLDER and SCIAMACHY overpasses. Pixels labeled cloud-free therefore are pixels that most likely remained cloud-free. Figure 4 shows that there are clear differences in behavior. Obviously, the scatter in the data labeled as cloudy is higher, which can be explained by the

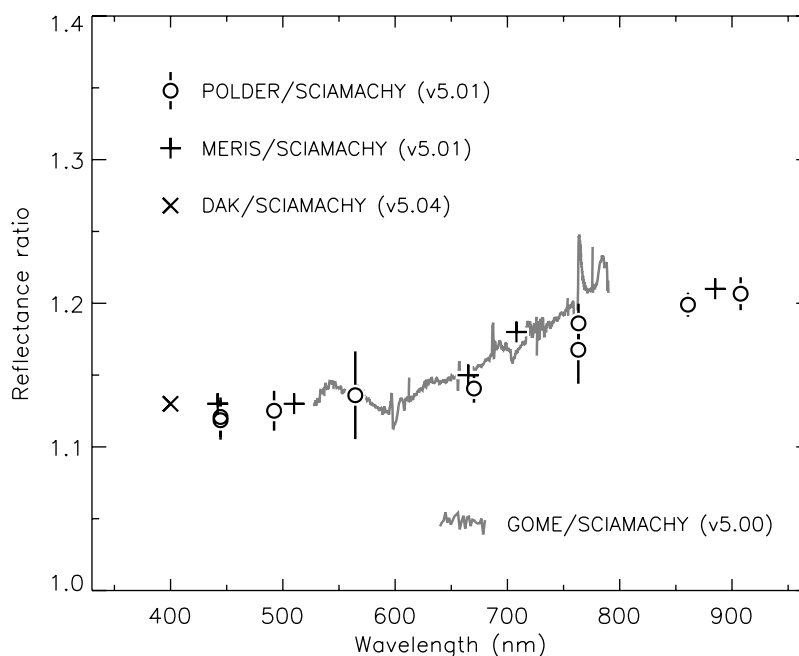


Figure 5. Ratio of the reflectances of POLDER and SCIAMACHY as a function of wavelength (indicated by circles). The ratios of SCIAMACHY reflectances w.r.t. two other satellite instruments (MERIS, GOME) are plotted as well, and a ratio based on comparisons with calculations by a radiative transfer code (DAK) in the UV. The SCIAMACHY data version numbers are also given.

unstable nature of these pixels in combination with the time difference between POLDER and SCIAMACHY overpasses.

[33] The linear fits were based on cloud-free data only because (1) we achieve a higher accuracy this way, (2) we want to avoid pixels which might suffer from scene changes caused by cloud movement in the time period between the overpasses of POLDER and SCIAMACHY, and (3) we automatically filter out reflectances over bright clouds which for some of the POLDER spectral channels (see Table 2) might cause saturation. We should mention that, as explained in section 3.4, for the 565- and 765-nm spectral bands, the SCIAMACHY pixels were larger to ensure a continuous spectrum over which to integrate equation (2). This explains why there are less data points and why the reported accuracy is lower. Additionally, we note that the measurement at 763 nm may be subject to a systematic error because for this channel, the integral in equation (2) includes a strong atmospheric absorption band (O_2 -A band).

[34] In Figure 5 we plotted the average ratios \bar{R}_i^P/R_i^S , for all nine POLDER spectral bands, determined from the linear fits in Figure 4, as a function of wavelength. The data points are indicated by circles. Error bars are given as well. They were based on the reported errors in the slopes of the linear fits presented in Figure 4. A first conclusion is that SCIAMACHY underestimates the Earth reflectance by 10–15% at blue wavelengths, by 15–20% at green/red wavelengths, and up to $\sim 20\%$ in the near-infrared.

[35] Also shown in Figure 5 are the results of inter-comparisons between SCIAMACHY and other sources. These sources include the satellite instruments GOME [Bovensmann *et al.*, 1999] and MERIS [Rast *et al.*, 1999], and the radiative transfer model DAK mentioned

before. The results, as indicated in Figure 5, can be found in the work of Tilstra *et al.* [2005], Acarreta and Stammes [2005], and Tilstra and Stammes [2006]. The different methods more or less agree with each other and with the new results from this paper. The maximum deviation is 5%, not much more than the reported accuracy of the instruments or techniques involved. One thing worth mentioning at this point is that the reflectance inter-comparison between MERIS and SCIAMACHY showed a noticeable nonlinear behavior for the smaller reflectances [Acarreta and Stammes, 2005]. In Figure 4 we found a clear linearity between the reflectances of POLDER and SCIAMACHY. This suggests that the nonlinearity found in the MERIS-SCIAMACHY intercomparison was not due to a nonlinearity present in the SCIAMACHY data.

4.2. Polarization

[36] The main result of the polarization comparison between the two instruments is shown in Figure 6. On the vertical axis of each plot, we have POLDER polarization data, which may be Q/I , U/I , or the degree of linear polarization P , measured by POLDER spectral bands 443P, 670P, or 865P. On the horizontal axis, we have Q/I , U/I , or P from SCIAMACHY PMDs 2, 3, or 4. The data originate from the scene shown in Figure 1 and were processed according to the method explained in section 3.5. In total, 1040 (forward scan) SCIAMACHY pixels were involved in the intercomparison, of which 807 were labeled cloud-free. Cloudy pixels are represented in Figure 6 by gray crosses, cloud-free pixels by black pluses. As before, backscan pixels were not included in the analysis. The intercomparison was performed for the lowest possible IT available in the SCIAMACHY data, which was 0.25 s for all pixels involved.

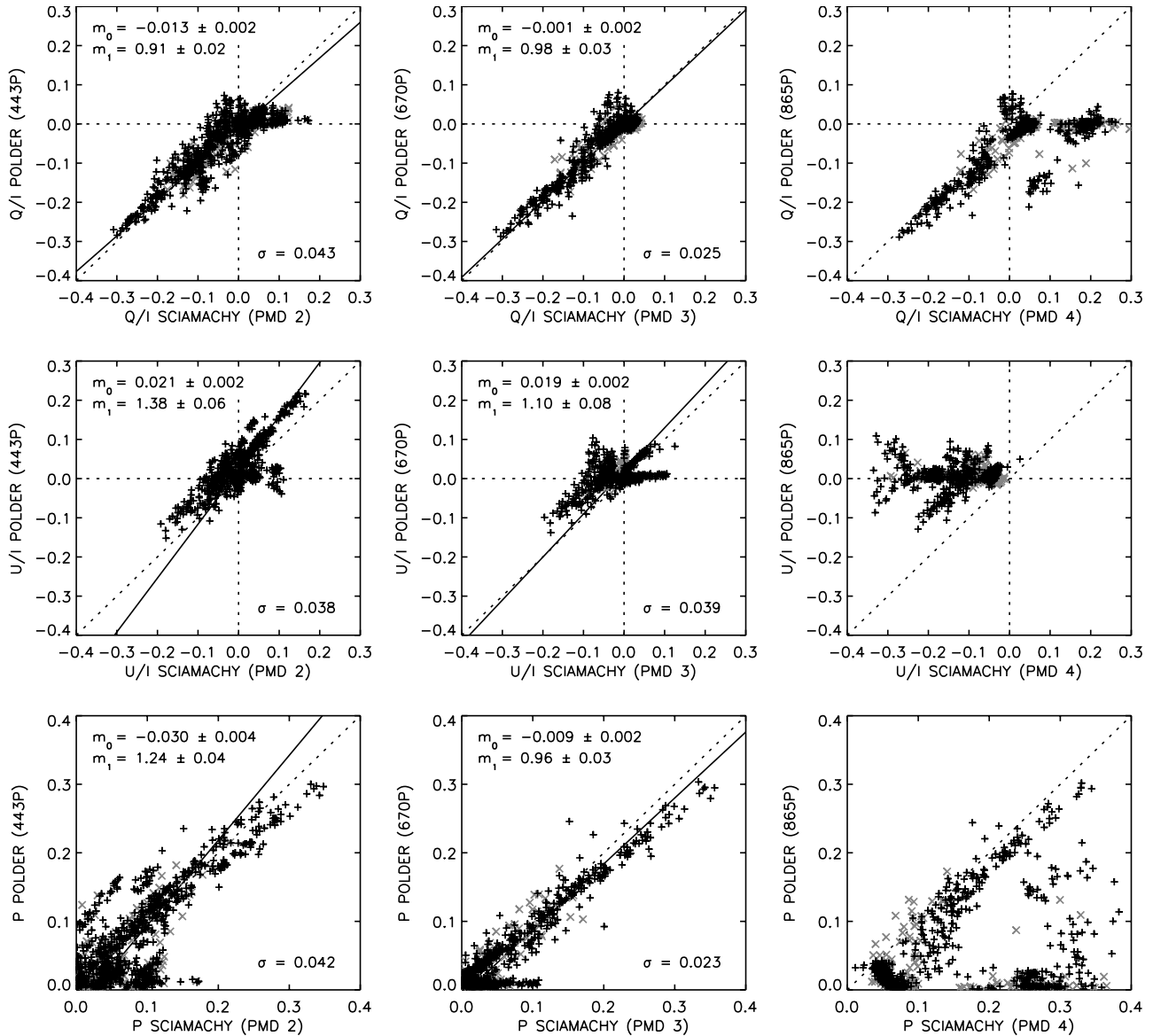


Figure 6. Stokes parameter ratios Q/I , U/I , and degree of linear polarization P , measured by POLDER, versus the same quantities measured by SCIAMACHY. Results are given for the three spectral bands that measure polarization. The gray crosses relate to cloudy pixels, the black pluses to pixels that were flagged cloud-free. The dotted lines indicate the origin and the one-to-one relationship. A linear two-parameter fit is presented for the data related to PMDs 2 and 3 (solid lines). The intercept m_0 and slope m_1 , and the errors in these, are given. The spread in the data is given by the standard deviation σ .

[37] The solid lines in Figure 6 are linear fits to the data. From earlier results, we know that the cloud-free data are more reliable; the linear fits were therefore fitted to these data only. The intercept m_0 and slope m_1 of the fits are given. The spread in the data was calculated and is presented, where useful, by the standard deviation σ . Starting out with the results for Q/I , we find a reasonable relationship between POLDER and SCIAMACHY for PMDs 2 and 3. The correlation is somewhat better for PMD 3, which is reflected by the linear fit, which has a slope closer to 1 (to be precise, 0.91 ± 0.02 for PMD 2 and 0.98 ± 0.03 for PMD 3). Also, the spread in the data (σ) is significantly less for PMD 3 than for PMD 2. Note that for both PMDs, the spread of the data points around the origin

(i.e., for unpolarized cases) is higher than elsewhere. As for Q/I from PMD 4, we must conclude that the SCIAMACHY data processor is failing to present the right values for a large number of data points. Note that despite the obvious problems, part of the PMD 4 data do show a similar correlation to the POLDER data as the other two PMDs.

[38] Looking at the U/I data, we see a different behavior. For PMD 2, the linear fit has a slope deviating strongly from one. The linear fit to the U/I data from PMD 3 also deviates from the one-to-one relationship. PMD 4 is again behaving the worst, with almost all values showing different behavior than POLDER. The data of the degree of linear polarization P emphasize that the data from PMD 3 are following POLDER better than the other two PMDs. For PMD 2,

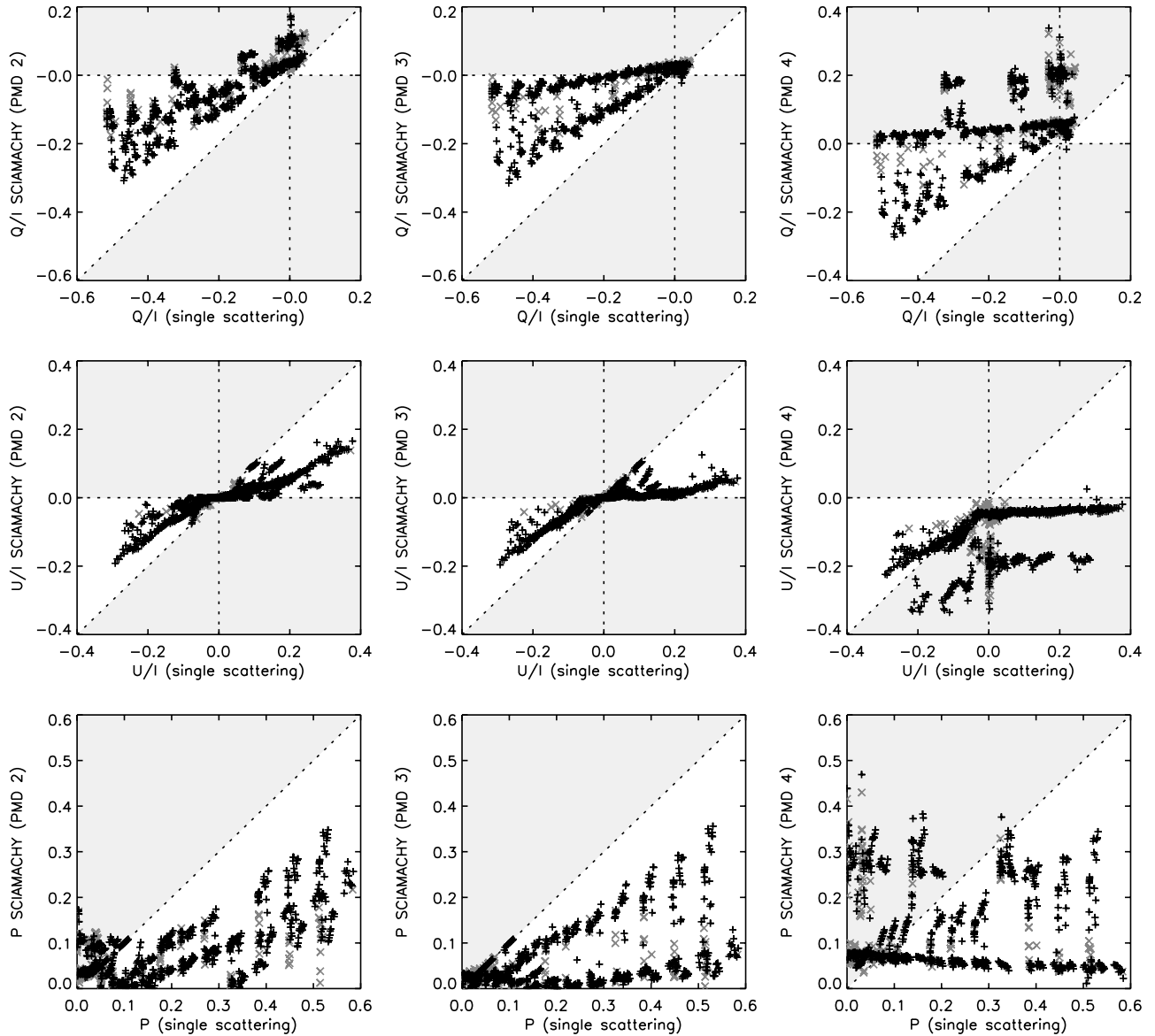


Figure 7. SCIAMACHY polarization quantities Q/I , U/I , and degree of linear polarization P , measured by PMDs 2, 3, and 4, versus the same quantities calculated for a Rayleigh single scattering atmosphere without surface reflection. Gray crosses relate to cloudy pixels, black pluses to cloud-free pixels. We distinguish between “likely” and “unlikely” domains in the scatterplot (see text). The “unlikely” domain is indicated by the gray color. For PMD 4, and to a lesser degree also for PMD 2, many data points are found in the “unlikely” regime.

the problems for unpolarized cases (where $P = 0$) are much clearer than before. Also, note the difference in σ between PMDs 2 and 3, again stressing the better results for PMD 3. The result for PMD 4 shows again that part of the data produce the right behavior, while many outliers are found as well.

[39] The accuracy of the POLDER polarization values was reported to be ~ 0.01 [Toubbé *et al.*, 1999], which leaves very little room for explaining the deviations found. In the SCIAMACHY data product, the reported errors for PMDs 2 and 3 are typically 0.01–0.02 for Q/I and 0.1–0.2 for U/I . For PMD 4, the reported errors are ~ 0.01 for Q/I and ~ 0.04 for U/I . Given the results from the polarization intercomparison, we must conclude that the reported errors in the SCIAMACHY data product are not representative for

the actual errors found in the polarization data because of insufficient quality of the polarization product present in SCIAMACHY data processor version 5.01.

[40] To further study the SCIAMACHY polarization data, we present in Figure 7 another way of analyzing polarization data. On the vertical axis of the plots, we present Q/I , U/I , or P , obtained from measurements by SCIAMACHY PMDs 2, 3, or 4. On the horizontal axis, we plot the same quantities, but now calculated for a Rayleigh single scattering atmosphere without surface reflection. Plots like these are very useful for a quick verification of the polarization data because for atmospheric polarization in normal cases, we should find $P < P_{ss}$ [see, e.g., Krijger *et al.*, 2005] and similar relations for Q/I and U/I . With these inequalities in mind, the nine scatterplots of Figure 7 can be divided into

two types of regions, one in which the polarization values are likely to be found (the “likely regime”), and one in which values are not expected to be found (the “unlikely regime,” which was given a gray color in Figure 7).

[41] Exceptions to this rule of thumb are found in sunglint and rainbow situations. However, for the present data, these situations should not occur, and we therefore do not expect a violation of this simple check, at least not for a significant part of the data. Starting with PMD 3, we find that most data points indeed do pass the sanity check, for Q/I , U/I , and P . For Q/I , however, the values near the origin of the plot slightly leave the likely regime, in a way that suggests that there may be an offset problem in the calculation of the Stokes parameter ratios. Also, U/I from PMD 3 clearly shows that some values with $P \sim 0$ (low-polarized cases) are found to be exactly equal to the single scattering value, which is a very unrealistic coincidence.

[42] When looking at Q/I and P for PMD 2, we find more data points than for PMD 3 violating the simple sanity check. This is especially the case for low-polarized situations (where $P \sim 0$). For PMD 4, the behavior is even more suspect, with more points in the unlikely regime, and more proof for “offset problems” in Q/I , U/I , and P . The plots shown in Figures 6 and 7 are in fact quite generic and were reproduced when focusing on other scenes than the one presented in Figure 1. We therefore conclude that the SCIAMACHY polarization data for PMD 3 are working for most cases, but that the polarization data from PMDs 2 and 4 are lacking quality.

5. Discussion and Interpretation of the Results

[43] The correlation between the SCIAMACHY and POLDER Earth reflectances, shown in Figure 4, is good: The internal spread of the data points around the linear fit (σ) is small, despite the fact that the individual data differ in geometry and scene type. For all wavelengths, there is, however, a systematic underestimation of the reflectance by SCIAMACHY by 10–20%, depending on wavelength. We attribute this to calibration problems of SCIAMACHY.

[44] As for the polarization comparison shown in Figure 6, the quantities derived from PMD 3 show a very reasonable agreement with those from POLDER’s polarization channel 670P, but for PMDs 2 and 4, the agreement is less good. Remarkably, there appear to be polarization data that behave as expected, while other data points show wrong values.

[45] Using the results from section 3.6, we now consider if the disagreements could be (partly) due to the spectral mismatch of the polarization bands of the two instruments. According to Figure 3, SCIAMACHY PMD 2 would always record a somewhat higher degree of linear polarization than POLDER spectral band 443P. However, according to Figure 6, and if we ignore the points around the origin which are clearly wrong, the POLDER values of P are just a little smaller than the SCIAMACHY value and not larger. So the spectral mismatch cannot be the cause the difference. Also, it should be mentioned that the presented simulations are quite pessimistic cases for estimating the effects of the spectral mismatch because polarizing aerosols were not included in the calculations. If they had been included, they would have flattened the curves in Figure 3 [see, e.g.,

Schutgens et al., 2004], thereby reducing the consequences of the mismatch between POLDER and SCIAMACHY polarization bands. Note also that for PMD 4, the mismatch is much smaller than for PMD 2, while the problems for PMD 4 are clearly larger. We therefore dismiss this spectral mismatch as a possible explanation for the disagreement between POLDER and SCIAMACHY in the polarization comparison.

[46] Instead, we find indications of what we called “offset problems” for all PMDs. This could point to a wrong calibration of the PMD signals. Also, we find that some of the data points are showing (numerically) the same value for U/I as the single scattering model. This is rather suspect. A plausible explanation for this phenomenon came to our attention recently. Because of the lower sensitivity of SCIAMACHY to Stokes parameter U , the retrieved U/I values are generally less reliable than the retrieved Q/I values. In fact, U/I values that after calculation are found to be in the “unlikely” regime [cf. section 4.2, where $U/I > (U/I)_{ss}$] are being set equal to the single scattering value $(U/I)_{ss}$ by the SCIAMACHY data processor (S. Slijkhuis, personal communication, 2006). However, this only explains the origin of the errors for a small fraction of the data points.

6. Summary and Conclusions

[47] In this paper, we presented new work on the validation of the radiometric calibration and polarization detection of the spectrometer SCIAMACHY. The validation relied on a careful comparison of the SCIAMACHY reflectance and polarization data with those of the imager POLDER. The POLDER instrument is well calibrated and, as such, may serve as a reliable reference for the actual Earth reflectance and polarization. More importantly, by virtue of the unique measurement design of POLDER, it is possible to find POLDER data that are able to mimic the SCIAMACHY observation geometry. This allows an accurate comparison.

[48] Our analysis clearly shows that SCIAMACHY systematically underestimates the Earth reflectance by as much as 10–20% in the wavelength range 400–1000 nm (software version 5.01). This outcome is supported by previous studies, based on different techniques, which provided comparable numbers. No dependence on viewing angle, latitude, longitude, scene, or instrument signal was found. In particular, we found no proof for a possible nonlinearity in the SCIAMACHY reflectance. All this combined leads us to conclude that the source of the current reflectance error is most likely an imperfect on-ground radiometric calibration of the instrument.

[49] The verification of the SCIAMACHY linear polarization for the first time revealed the magnitude of the error of the SCIAMACHY polarization data from PMDs 2, 3, and 4. For PMD 3, and to a lesser degree also PMD 2, the polarization quantities are of reasonable quality. We find, however, that SCIAMACHY’s polarization product is seriously lacking quality for PMD 4. To illustrate the impact of the current state of the polarization on the reflectance, the typical polarization errors encountered in Figure 6, reflected by the standard deviation σ for PMD 2/3 and by a bias of ~ 0.1 for PMD 4, would lead to errors in the reflectance of 2% at 500 nm, 1% at 700 nm, to 3% at 900 nm.

[50] In conclusion, the current SCIAMACHY level-1 data (software version 5.01) suffer from calibration errors. This applies to both the radiance and polarization products. The approach of this study may also be interesting for the validation of new polarization measuring satellite instruments, such as Polarization and Anisotropy of Reflectances for Atmospheric Sciences coupled with Observations from a Lidar (PARASOL), GOME-2 on the MetOp satellite, launched on 19 October 2006, and Aerosol Polarimetry Sensor (APS) on the future Glory mission.

[51] **Acknowledgments.** The work presented in this publication was financed by the Netherlands Agency for Aerospace Programmes (NIVR) and the Space Research Organisation Netherlands (SRON) through project EO-076. We would like to thank the Centre National d'Etudes Spatiales (CNES) and the Japan Aerospace Exploration Agency (JAXA) for providing the POLDER data. The European Space Agency (ESA) and the Deutsches Zentrum für Luft- und Raumfahrt (DLR) are acknowledged for providing the SCIAMACHY data. Further, we would like to thank S. Slijkhuis for stimulating discussions.

References

- Aben, I., C. P. Tanzi, W. Hartmann, D. M. Stam, and P. Stammes (2003), Validation of space-based polarization measurements by use of a single-scattering approximation, with application to the Global Ozone Monitoring Experiment, *Appl. Opt.*, *42*(18), 3610–3619.
- Acarreta, J. R., and P. Stammes (2003), Verification of SCIAMACHY's Reflectance over the Sahara, in Proceedings of the Envisat Validation Workshop, *Eur. Space Agency Spec. Publ. SP-531*, edited by H. Sawaya-Lacoste, ESA Publications Division, Frascati, Italy.
- Acarreta, J. R., and P. Stammes (2005), Calibration comparison between SCIAMACHY and MERIS onboard ENVISAT, *IEEE Geosci. Remote Sens. Lett.*, *2*(1), 31–35, doi:10.1109/LGRS.2004.838348.
- Acarreta, J. R., P. Stammes, and W. H. Knap (2004), First retrieval of cloud phase from SCIAMACHY spectra around 1.6 micron, *Atmos. Res.*, *72*, 89–105.
- Bovensmann, H., J. P. Burrows, M. Buchwitz, J. Frerick, S. Noël, V. V. Rozanov, K. V. Chance, and A. P. H. Goede (1999), SCIAMACHY: Mission objectives and measurement modes, *J. Atmos. Sci.*, *56*(2), 127–150.
- Bowker, D. E., R. E. Davis, D. L. Myrick, K. Stacy, and W. T. Jones (1985), Spectral reflectances of natural targets for use in remote sensing studies, *NASA Ref. Publ.* 1139, 184 pp., NASA Langley Res. Cent., Hampton, Va.
- Burrows, J. P., et al. (1999), The Global Ozone Monitoring Experiment (GOME): Mission concept and first scientific results, *J. Atmos. Sci.*, *56*(2), 151–175.
- de Graaf, M., and P. Stammes (2005), SCIAMACHY Absorbing Aerosol Index—Calibration issues and global results from 2002–2004, *Atmos. Chem. Phys.*, *5*, 2385–2394.
- de Haan, J. F., P. B. Bosma, and J. W. Hovenier (1987), The adding method for multiple scattering calculations of polarised light, *Astron. Astrophys.*, *183*, 371–391.
- Deschamps, P.-Y., F.-M. Bréon, M. Leroy, A. Podaire, A. Brickaud, J.-C. Buriez, and G. Sèze (1994), The POLDER mission: Instrument characteristics and scientific objectives, *IEEE Trans. Geosci. Remote Sens.*, *32*(3), 598–615, doi:10.1109/36.297978.
- Gottwald, M. et al. (2006), SCIAMACHY—Monitoring the changing Earth's atmosphere, 176 pp., DLR-IMF, Oberpfaffenhofen, Germany.
- Hagolle, O., P. Goloub, P.-Y. Deschamps, H. Cosnefroy, X. Briottet, T. Bailleul, J.-M. Nicolas, F. Parol, B. Lafrance, and M. Herman (1999), Results of POLDER in-flight calibration, *IEEE Trans. Geosci. Remote Sens.*, *37*(3), 1550–1566, doi:10.1109/36.7632661999.
- Hasekamp, O. P., J. Landgraf, and R. van Oss (2002), The need of polarization modeling for ozone profile retrieval from backscattered sunlight, *J. Geophys. Res.*, *107*(D23), 4692, doi:10.1029/2002JD002387.
- Hoogen, R., V. V. Rozanov, and J. P. Burrows (1999), Ozone profiles from GOME satellite data: Algorithm description and first validation, *J. Geophys. Res.*, *104*(D7), 8263–8280, doi:10.1029/1998JD100093.
- Koelemeijer, R. B. A., P. Stammes, J. W. Hovenier, and J. F. de Haan (2001), A fast method for retrieval of cloud parameters using oxygen a band measurements from the Global Ozone Monitoring Experiment, *J. Geophys. Res.*, *106*(D4), 3475–3490, doi:10.1029/2000JD900657.
- Krijger, J. M., and L. G. Tilstra (2003), Current status of SCIAMACHY's polarisation measurements, in Proceedings of the Envisat Validation Workshop, *Eur. Space Agency Spec. Publ. SP-531*, edited by H. Sawaya-Lacoste, ESA Publications Division, Frascati, Italy.
- Krijger, J. M., C. P. Tanzi, I. Aben, and F. Paul (2005), Validation of GOME polarization measurements by method of limiting atmospheres, *J. Geophys. Res.*, *110*, D07305, doi:10.1029/2004JD005184.
- Meijer, Y. J., R. J. van der A, R. F. van Oss, D. P. J. Swart, H. M. Kelder, and P. V. Johnston (2003), Global Ozone Monitoring Experiment ozone profile characterization using interpretation tools and lidar measurements for intercomparison, *J. Geophys. Res.*, *108*(D23), 4723, doi:10.1029/2003JD003498.
- Munro, R., R. Siddans, W. J. Reburn, and B. J. Kerridge (1998), Direct measurements of tropospheric ozone distributions from space, *Nature*, *392*, 168–171.
- Platt, U. (1994), Differential Optical Absorption Spectroscopy (DOAS), in *Air Monitoring by Spectroscopic Techniques*, Chemical Analysis Series, vol. 127, edited by M. W. Sigrist pp. 27–84, John Wiley and Sons.
- Rast, M., J. L. Bezy, and S. Bruzzi (1999), The ESA Medium Resolution Imaging Spectrometer MERIS—A review of the instrument and its mission, *Int. J. Remote Sens.*, *20*, 1681–1702.
- Schutgens, N. A. J., L. G. Tilstra, P. Stammes, and F.-M. Bréon (2004), On the relationship between Stokes parameters Q and U of atmospheric ultraviolet/visible/near-infrared radiation, *J. Geophys. Res.*, *109*, D09205, doi:10.1029/2003JD004081.
- Skupin, J., S. Noël, M. W. Wuttke, H. Bovensmann, and J. P. Burrows (2003), Calibration of SCIAMACHY in-flight measured irradiances and radiances—First results of level 1 validation, in Proceedings of the Envisat Validation Workshop, *Eur. Space Agency Spec. Publ. SP-531*, edited by H. Sawaya-Lacoste, ESA Publications Division, Frascati, Italy.
- Slijkhuis, S. (2001), SCIAMACHY level 0 to 1c processing algorithm theoretical basis document, Tech. Note ENV-ATB-DLR-SCIA-0041, Dtsch. Zent. für Luft- und Raumfahrt, Oberpfaffenhofen, Germany.
- Spurr, R. J. D. (2001), Linearized radiative transfer theory: A general discrete ordinate approach to the calculation of radiances and analytic weighting functions, with application to atmospheric remote sensing. Ph.D. thesis, Tech. Univ. Eindhoven, The Netherlands.
- Stammes, P. (2001), Spectral radiance modelling in the UV-visible range, in *IRS 2000: Current Problems in Atmospheric Radiation*, edited by W. L. Smith and Y. M. Timofeyev, pp. 385–388, Deepak, A., Hampton, Va.
- Tilstra, L. G., and P. Stammes (2005), Alternative polarisation retrieval for SCIAMACHY in the ultraviolet, *Atmos. Chem. Phys.*, *5*, 2099–2107.
- Tilstra, L. G., and P. Stammes (2006), Intercomparison of reflectances observed by GOME and SCIAMACHY in the visible wavelength range, *Appl. Opt.*, *45*(17), 4129–4135.
- Tilstra, L. G., G. van Soest, and P. Stammes (2005), Method for in-flight satellite calibration in the ultraviolet using radiative transfer calculations, with application to Scanning Imaging Absorption Spectrometer for Atmospheric Chartography (SCIAMACHY), *J. Geophys. Res.*, *110*, D18311, doi:10.1029/2005JD005853.
- Toubbé, B., T. Bailleul, J.-L. Deuze, P. Goloub, O. Hagolle, and M. Herman (1999), In-flight calibration of the POLDER polarized channels using the Sun's glitter, *IEEE Trans. Geosci. Remote Sens.*, *37*(1), 513–524, doi:10.1109/36.739104.
- van de Hulst, H. C. (1981), *Light Scattering by Small Particles*, Dover, Mineola, N. Y.
- van der A, R. J., R. F. van Oss, A. J. M. Pijters, J. P. F. Fortuin, Y. J. Meijer, and H. M. Kelder (2002), Ozone profile retrieval from recalibrated Global Ozone Monitoring Experiment data, *J. Geophys. Res.*, *107*(D15), 4239, doi:10.1029/2001JD000696.
- van Soest, G., L. G. Tilstra, and P. Stammes (2005), Large-scale validation of SCIAMACHY reflectance in the ultraviolet, *Atmos. Chem. Phys.*, *5*, 2171–2180.
- von Hoyningen-Huene, W., A. A. Kokhanovsky, M. W. Wuttke, M. Buchwitz, S. Noël, K. Gerilowski, J. P. Burrows, B. Latter, R. Siddans, and B. J. Kerridge (2006), Validation of SCIAMACHY top-of-atmosphere reflectance for aerosol remote sensing using MERIS L1 data, *Atmos. Chem. Phys. Disc.*, *6*, 673–699.

L. G. Tilstra and P. Stammes, Royal Netherlands Meteorological Institute, P.O. Box 201, NL-3730 AE, De Bilt, The Netherlands. (tilstra@knmi.nl; stammes@knmi.nl)